Catalysis Science & Technology

ROYAL SOCIETY OF CHEMISTRY

PAPER

View Article Online
View Journal | View Issue

Cite this: *Catal. Sci. Technol.*, 2020, 10, 5487

A nitrogen-doped carbon-coated silicon carbide as a robust and highly efficient metal-free catalyst for sour gas desulfurization in the presence of aromatics as contaminants†

Cuong Duong-Viet,[ab] Jean-Mario Nhut,[a] Tri Truong-Huu,[c] Giulia Tuci,[d] Lam Nguyen-Dinh,[c] Yuefeng Liu, *[e] Charlotte Pham,[f] Giuliano Giambastiani *[adg] and Cuong Pham-Huu*[a]

As far as environmental chemistry is concerned, N-doped nanocarbons have been employed as efficient, selective and robust metal-free systems for the selective oxidation of H_2S to elemental sulfur in tail gas treatment units. Modified Claus units that include tail gas treatments can reach up to 99.9% conversion of H_2S into elemental sulfur, a technology that matches well with the more and more challenging environmental concerns. Contaminants in the feed stream include hydrocarbons whose incomplete upstream removal may pose several problems to the catalytic units of a modified Claus reactor. Indeed, when hydrocarbons meet catalysts, they may undergo degradation processes that typically cause catalyst poisoning and make necessary its frequent regeneration if not its complete substitution. This contribution describes a straightforwardly prepared mesoporous N-doped carbon coating for SiC extrudates, offering the excellent desulfurization performance of the corresponding composite (N–C/SiC) along with its remarkably high resistance towards deactivation/fouling in the presence of relatively high concentrations of toluene [1000 ppm ≤ [tol] ≤ 20 000 ppm] as aromatic contaminant. The study has unveiled the existence of a positive "solvent effect" played by toluene on the process selectivity when N–C/SiC is used as a catalyst while confirming at the same time the remarkably high H_2S conversion rates and resistance to deactivation of the metal-free system under harsh reaction conditions.

Received 8th May 2020,
Accepted 5th July 2020

DOI: 10.1039/d0cy00945h

rsc.li/catalysis

Introduction

Natural gas is in the third place among fossil fuels for energy applications and its use is steadily growing compared to other fossil energy sources such as petroleum and charcoal.[1,2] However, natural gas contains sulfur compounds that constitute a source of concern because of their corrosive nature as well as their potential hazard to human health and the environment. In addition, sulfur species may deeply affect the performance and lifetime of catalysts in processes where natural gas is employed as a chemical reagent; their presence, even in traces, can inhibit or destroy catalysts used in gas processing. For these reasons, S compound removal from natural gas streams is of utmost importance before any gas manipulation/processing.[3–5] The most widely used technology applied nowadays to this purpose is the Claus process,[5] which allows recovering elemental sulfur from S-containing gases through a complex sequence of thermal and catalytic transformations, where H_2S conversion/removal typically reaches 96–98%, depending on the feed composition and the thermodynamic limitations of the process. In modified Claus units, a tail gas treatment is included at the end of the process (direct oxidation with no thermodynamic limitations) that makes possible an almost complete (up to 99.9%) hydrogen sulfide conversion into elemental sulfur, hence

[a] *Institute of Chemistry and Processes for Energy, Environment and Health (ICPEES), UMR 7515 CNRS, Université de Strasbourg, 25 rue Becquerel, 67087 Strasbourg Cedex 02, France. E-mail: giambastiani@unistra.fr, cuong.pham-huu@unistra.fr*
[b] *Ha-Noi University of Mining and Geology, 18 Pho Vien, Duc Thang, Bac Tu Liem, Ha-Noi, Vietnam*
[c] *The University of Da-Nang, University of Science and Technology, 54, Nguyen Luong Bang, Da-Nang, Vietnam*
[d] *Institute of Chemistry of OrganoMetallic Compounds, ICCOM-CNR and Consorzio INSTM, Via Madonna del Piano, 10 – 50019, Sesto F.no, Florence, Italy. E-mail: giuliano.giambastiani@iccom.cnr.it*
[e] *Dalian National Laboratory for Clean Energy (DNL), Dalian Institute of Chemical Physics, Chinese Academy of Science, 457 Zhongshan Road, 116023 Dalian, China. E-mail: yuefeng.liu@dicp.ac.cn*
[f] *SICAT SARL, 20 place des Halles, 67000 Strasbourg, France*
[g] *Kazan Federal University, 420008 Kazan, Russian Federation*

† Electronic supplementary information (ESI) available. See DOI: 10.1039/d0cy00945h

minimizing SO_2 emissions from the incinerator.[6] The tail gases of the Claus process may contain 0.4–1.5 vol% H_2S and up to 40% water vapour.[7] Besides facing highly environmental concerns, selective H_2S oxidation allows conversion of a harmful species into commercially valuable products. Indeed, sulfur is a highly interesting compound for industry with applications that span from the production of fertilizers for crops to base materials used in construction and in chemistry fields. About 75 Mt of elemental sulfur are globally produced per year from oil and gas processing units which contribute to a large economic area.[8]

Gaseous streams from traditional refineries also contain other contaminants such as methanol, heavy hydrocarbons, and aromatics [*i.e.* benzene, toluene and xylene (BTX)] as well as N-containing compounds.[9] Some of these impurities are known to deeply (and detrimentally) impact on the life cycle of catalysts applied to sulfur recovery in dedicated reactor units. Among these, BTX (C $\geq$7 in particular) are responsible for the generation of carbonaceous or heavy carbon–sulfur compounds under desulfurization conditions.[10] Their incomplete removal from upstream thermal gas treatment often translates into catalyst fouling phenomena that invariably affect the process performance or in worse cases can cause complete catalyst deactivation.

Reduction of BTX concentration in acid gas streams has been approached through various technological solutions whose practical exploitation invariably increases the process complexity as well as that of the reactor setup. Amine or solvent enrichment units (acid gas enrichment (AGE) units)[11] used to obtain higher hydrogen sulfide concentrations in the stream allow one to perform a sour gas thermal treatment [before it reaches the catalytic desulfurization unit (SRU)] at higher temperature.[12] In this way, an almost complete hydrocarbon combustion can be achieved. Nevertheless, besides the higher reactor scheme complexity, the introduction of liquids into the process translates into higher operational and energy costs for the periodical regeneration of the absorbers. Another method for removing BTX from acid gases is to install activated carbon beds upstream of the desulfurization unit (SRU) for absorbing BTX fractions.[13] Although the long-term stability of carbon guard beds remains a matter of debate within the scientific community, they certainly require frequent regeneration treatments to remove absorbed products. This regeneration phase typically changes the feed conditions to the Claus unit or it can even determine the complete feed shutdown. In addition, the installation of washing equipment for the absorbers' regeneration as well as the downstream treatment of BTX-contaminated wastewaters is required. Finally, BTX oxidation by SO_2 before they come in contact with the catalyst bed of a Claus reactor represents a possible solution to the problem, an approach that has been thoroughly investigated mainly on a theoretical ground.[14–16]

Therefore, robust and durable catalysts suitable for the selective oxidation of H_2S under variable acid concentrations and featuring excellent resistance to aromatic deactivation are highly desirable and remain a challenging subject of research.

In the past decades, carbon-based (nano)materials, *i.e.* nanotubes (CNTs) and nanofibers (CNFs) or thin-carbon film deposits (in the form of pure carbons or light-hetero-doped materials), have received increasing interest from the catalysis community as either versatile supports for various metal active phases or highly efficient and single-phase metal-free systems to be employed in a wide series of relevant catalytic transformations.[17,18]

In particular, N-doped nanocarbons are recognized as excellent metal-free catalytic materials for a wide series of key processes, often exhibiting improved performance and higher long-term stability compared to their traditional (and metal-based) counterparts. They have successfully been employed for the selective and highly efficient alkane dehydrogenation to alkenes within direct (DDH) or oxidative dehydrogenation (ODH) schemes[19,20] as catalytic materials for selective oxidation reactions,[21–24] as electrocatalysts for small molecule activation and reduction (ORR, HER, CO_2RR)[25–28] or as promoters in other challenging catalytic transformations.[29,30] Although the role of N-doping in metal-free catalysts depends on the material's downstream application, it is generally accepted that the introduction of electron-rich elements in a pure carbon network redraws its chemico-physical (and morphological) properties and tunes the material's ability to interact with external molecules/reagents. As far as environmental chemistry is concerned, N-doped nanocarbons have also been reported as highly efficient metal-free systems for the selective oxidation of H_2S from tail gases to elemental sulfur.[22,31–39] N-doped C-nanomaterials as catalysts have a number of technical advantages compared to classical metal-based systems that go beyond their already excellent performance. They generally are single-phase systems that prevent classical leaching or sintering deactivation phenomena typically encountered in metal nanoparticle-based catalysts. As metal-free systems, they largely prevent catalyst fouling phenomena and represent a cheaper and sustainable tool for industrially relevant processes. In addition, their typical basic character largely prevents the occurrence of undesired cracking reactions often responsible for the rapid catalyst fouling. We have recently proposed a "greener" and highly versatile synthetic technology to the preparation of N-doped carbon-based composites starting from food-grade raw components.[21,32,40] Besides offering an unconventional protocol to the preparation of highly N-doped carbon phases with controlled macro- and microscopic shapes, such a technology simplifies the doping procedure and reduces the formation of toxic by-products typically encountered under more traditional chemical-vapor-deposition (CVD)-based synthetic schemes.

In this report, silicon carbide (SiC) extrudates coated with a mesoporous N-doped-carbon phase (N–C/SiC) have been investigated as durable and highly efficient metal-free catalysts for H_2S oxidation from a sour gas containing toluene [selected as the probe molecule for aromatic (BTX)

impurities] at variable concentrations. We demonstrate how catalysts with basic surface properties are ideal candidates for the highly efficient and selective H_2S desulfurization under severe reaction conditions (0.5 vol% ≤ [H_2S] ≤ 2 vol%; 1000 ppm ≤ [tol] ≤ 20 000 ppm).[41]

To accomplish our purposes, silicon carbide (SiC) has been selected as the matrix for the N–C active phase due to its high mechanical resistance together with high thermal[42] and chemical stability under aggressive acidic/oxidative or basic environments that make it an ideal choice as a catalyst support across many industrially relevant heterogeneous transformations.[33,43,44] Moreover, it is commercially available in different sizes and shapes (Fig. S1†) and possesses a high chemical inertness together with a medium thermal conductivity that may reduce or even prevent the generation of local temperature gradients (hot spots) within the catalyst bed while operating highly exothermic transformations.[45] In contrast with more common and micro-/mesoporous metal-oxide supports for catalysis (*i.e.* γ-Al_2O_3, SiO_2), this ceramic is commercially provided as an open cell meso-/macroporous network. This property ensures an ideal diffusion of reagents and intermediates through the catalyst bed, avoids pressure drops in packed bed reactors and limits product residence time within the catalyst bed with a better subsequent process selectivity control. In addition, the treatment of spent SiC-based catalysts with aggressive and oxidative reagents can be used to remove the deposited active phases, thus recovering pristine supports for reuse.

At odds with more classical metal-based catalysts, the N–C/SiC composite has shown excellent desulfurization performance with remarkably high resistance towards catalyst deactivation/fouling even in the presence of 5000 ppm of toluene. In addition, a positive "solvent effect" played by toluene in the reagents' gas stream has been observed in terms of process selectivity with an increased elemental sulfur rate of up to 30% compared to selectivity values recorded for the same metal-free catalyst operated under identical but toluene-free conditions. A complete screening of N–C/SiC performance in H_2S desulfurization catalysis under variable conditions (0.5 vol% ≤ [H_2S] ≤ 2 vol%; 1000 ppm ≤ [tol] ≤ 20 000 ppm; GHSVs from 1200 h^{-1} to 2400 h^{-1}), including catalyst oxidative/regeneration treatments, has been systematically discussed. In addition, N–C/SiC performance has been compared with that of the benchmark Fe_2O_3/SiO_2 catalyst[46] for the sake of completeness.

Materials and methods

Materials and characterization methods

Silicon carbide (SiC) was purchased from Sicat SARL (www.sicatcatalyst.com) in the form of mesoporous pellets (2 × 1 mm, $h \times \varnothing$)[47–49] with a specific surface area (SSA) of 25 ± 1 $m^2\ g^{-1}$ measured by N_2 physisorption (at 77 K). Extra-pure ammonium carbonate [$(NH_4)_2CO_3$, MW: 96.09 g mol^{-1}; lot: A0356079], D-glucose 100% [$C_6H_{12}O_6$, MW: 180.16 g mol^{-1}] and citric acid [$C_6H_8O_7$ anhydrous, ≥99.5%, MW: 192.12 g mol^{-1}] were provided by ACROS Organic™, MYPROTEIN™ and VWR Chemicals, respectively. Unless otherwise stated, all reagents and solvents were used as provided by commercial suppliers without any further purification/treatment. Scanning electron microscopy (SEM) was carried out on an UHR-SEM Gaia 3 FIB/SEM (TESCAN). The electron beam used for SEM imaging was of 10 kV operating in high-vacuum mode using BSE and SE detectors. EDX semi-quantitative analyses were conducted on an EDS X-ray microanalysis system (EDAX, AMETEK, USA), TEAM™ EDS Basic Software Suite. Samples were deposited onto a double face graphite tape in order to avoid a charging effect during the analysis. Transmission electron microscopy (TEM) measurements were acquired on a JEOL 2100F instrument operating at 200 kV, equipped with a GATAN Tridiem imaging filter and an aberration corrected condenser. Electron energy-loss spectroscopy (EELS) analyses were performed in the scanning mode (STEM) with a 30 mrad convergence angle and a 25 mrad collection angle. The spectral images were acquired in 20 × 33 pixels with an exposure time of 1 s for each pixel. The energy resolution was 1.7 eV. Elemental signals were extracted from the Si–L, C–K, N–K and O–K edges. Energy-filtered TEM (EFTEM) measurements were acquired using a three-window method with energy slits of 8, 30 and 20 eV and acquisition times of 10 s, 30 s and 40 s for Si, C and N, respectively. N_2 adsorption–desorption measurements were carried out on a Micromeritics® sorptometer at liquid N_2 temperature and relative pressures between 0.06 and 0.99 P/P_0. Each sample was outgassed at 250 °C under ultra-high vacuum for 8 h prior to analysis in order to desorb moisture and adsorbed volatile species. X-ray photoelectron spectroscopy (XPS) was carried out in an ultrahigh vacuum (UHV) spectrometer equipped with a CLAM4 (MCD) hemispherical electron analyzer. The Al Kα line (1486.6 eV) of a dual anode X-ray source was used as incident radiation. Survey and high-resolution spectra were recorded in constant pass energy mode (100 and 20 eV, respectively). The CASA XPS program with a Gaussian–Lorentzian mix function and Shirley background subtraction was employed to deconvolute XPS spectra. Elemental analyses were performed on a Thermo FlashEA 1112 Series CHNS-O analyzer, and elemental average values were calculated over three independent runs. Powder diffraction (PXRD) measurement was carried out on a Bruker D-8 Advance diffractometer equipped with a Vantec detector (Cu Kα radiation) working at 40 kV and 40 mA. X-ray diffractograms were recorded in the 10–80° 2θ region at room temperature in air. Iron loading for Fe_2O_3 catalyst was fixed using inductively coupled plasma atomic emission spectrophotometry (ICP-AES) after acidic mineralization of the Fe/SiO_2 sample using an Optima 2000 Perkin Elmer inductively coupled plasma (ICP) Dual Vision instrument. Thermogravimetric analyses were performed in air (50 mL min^{-1}) from 40 to 900 °C (heating rate: 10 °C min^{-1}) on an EXSTAR Seiko 6200 analyser. Acid–base titration was accomplished using the following procedure:[28,50–53] 10 mg of N–C/SiC were suspended in 7 mL of a standardized HCl

solution (3×10^{-3} M, standardized with Na_2CO_3 as primary standard) and stirred at room temperature for 48 h. After that, three aliquots of the solution were titrated with a standardized NaOH solution (2.5×10^{-3} M). The basic site loading was finally calculated as the average value over three independent titration runs.

Synthesis of N–C/SiC catalysts

Commercial SiC in the form of extrudates [($\varnothing_{OD}$) ≈1 mm × (L, length) ≈2 mm] was thoroughly washed with deionized water in order to remove powdery material fractions; then it was dried at 130 °C overnight. The N–C/SiC catalyst was then prepared by adapting and improving our previous procedures[21,32,40] to obtain a highly nitrogen-doped carbon thin layer at the SiC outer surface. In a typical procedure, 1.5 g of D-glucose and 2.25 g of citric acid were added to 10 mL of ultrapure Milli-Q water at room temperature. Afterwards, 1.73 g of ammonium carbonate were added portion-wise to the stirred solution maintained at room temperature (a copious effervescence due to CO_2 evolution was observed during this phase). The as-prepared solution was used as a pre-catalytic phase for the soaking/impregnation of 10 g of SiC extrudates.[40] Wet solids underwent the following thermal treatments. SiC impregnated with 5 mL of the above-mentioned solution was maintained at 40 °C up to dryness before being heated in air at 130 °C for 1 h (heating rate 10 °C min^{-1}). During this phase a thin pre-catalytic coating of the SiC matrix, essentially made of D-glucose and basic ammonium citrate, is formed.[21,32] The resulting solid was then calcined at 400 °C for 2 h (heating rate 2 °C min^{-1}) to obtain a first N-doped mesoporous C-phase coating. The as-prepared composite underwent a second soaking/impregnation treatment using the remaining (5 mL) pre-catalyst solution.

The wet solid was dried again at 40 °C before repeating the calcination steps in air at 130 (1 h) and 400 °C (2 h). The composite was then treated at 900 °C (heating rate: 10 °C min^{-1}) under an inert atmosphere (He) for 2 h (annealing) during which the mesoporous N-doped graphitized C-coating for the SiC matrix was formed.

Fe_2O_3/SiO_2 (2.6 wt% Fe) was synthesized according to literature procedures[46] and employed as a benchmark system for H_2S desulfurization of sour gases under conditions identical to those (hard) operated with our metal-free composite (see Fig. S2† for the XRD spectrum of the iron catalyst).[54] Fe_2O_3/SiO_2 was prepared by incipient wetness impregnation of 10 g of SiO_2 powder with an aqueous solution of iron nitrate [$Fe(NO_3)_3 \cdot 9H_2O$, MW: 404.00 g mol^{-1}] obtained by dissolving 2.23 g of the iron(III) salt in 10 mL of ultrapure Milli-Q water at room temperature. After the solid was dried at 130 °C overnight, it was calcined in air at 350 °C (heating rate of 5 °C min^{-1}) and maintained at the target temperature for 2 h before being used as such in catalysis. The final iron loading was measured by ICP-AES analysis and it was fixed at 2.6 wt%.

Selective H_2S oxidation to elemental sulfur

The H_2S oxidation process can be outlined according to the following main equations (eqn (1)–(3)). In the present study, H_2S selective oxidation to elemental sulfur (eqn (1)) was promoted by a N–C/SiC catalyst located within a glass tubular reactor working isothermally under atmospheric pressure. A representation of the desulfurization scheme is given in Fig. S3 of the ESI.†[55,56]

$$2H_2S + O_2 \rightarrow 2S + 2H_2O \quad \Delta H = -187 \text{ kJ mol}^{-1} \tag{1}$$

$$S + O_2 \rightarrow SO_2 \quad \Delta H = -297 \text{ kJ mol}^{-1} \tag{2}$$

$$2H_2S + 3O_2 \rightarrow 2SO_2 + 2H_2O \quad \Delta H = -518 \text{ kJ mol}^{-1} \tag{3}$$

To this aim, 6 g of N–C/SiC (V_{cat} 7.5 cm^3) were loaded on a silica wool pad located in a tubular Pyrex reactor ($\varnothing_{ID}$: 16 mm) and housed in a vertical tubular electrical furnace. The furnace temperature was controlled using a K-type thermocouple and a Minicor regulator. The reactant gas mixture [H_2S (1 vol%), O_2 (2.5 vol%), H_2O (30 vol%) in inert He as carrier (balance)] was passed downward through the catalyst bed, with gas flow rates monitored through Brooks 5850TR mass flow controllers. Steam (30 vol%) in the reactant feed was ensured by bubbling the inert carrier in a saturator containing hot water at 80 °C. **CAUTION!** *H_2S is a colourless, flammable, highly toxic gas. It must be handled – including its solutions – rigorously under a fume hood and with all necessary precautions.* The gas hourly space velocity (GHSV) was fixed at either 1200 or 2400 h^{-1} (corresponding to 150 and 300 mL min^{-1}, respectively) and the O_2-to-H_2S molar ratio was kept constant at 2.5. The reaction rate (λ) was calculated as mmol H_2S_{conv} g_{cat}^{-1} h^{-1}. The influence of toluene on the catalyst performance was investigated by feeding the reactant stream with toluene vapours at variable concentrations [from 0.1 vol% (1000 ppm) up to 2.0 vol% (20 000 ppm)]. Toluene was fed in the stream by passing a He flow through a saturator containing pure toluene constantly maintained at 40 °C. To this purpose, an independent line of He (Fig. S3†) was used to feed toluene in the reagent stream and its target concentration was adjusted by regulating the flow of the carrier. The amount of toluene passing through the catalyst was double-checked by measuring the real liquid volume of toluene vaporized per day of experiment. All catalytic runs were carried out in continuous mode. Hence, most of the formed elemental sulfur was vaporized (because of the high partial pressure of sulfur at the target reaction temperatures) and condensed alongside with steam at the reactor outlet in a trap maintained at room temperature. The analysis of the inlet and outlet gases was performed online using a Varian CP-3800 gas chromatograph (GC) equipped with a Chrompack CP SilicaPLOT capillary column and a thermal catharometer detector (TCD) for the detection of O_2, H_2S, H_2O and SO_2. H_2S and SO_2 concentrations were recalculated on the basis of the corrected flow after steam

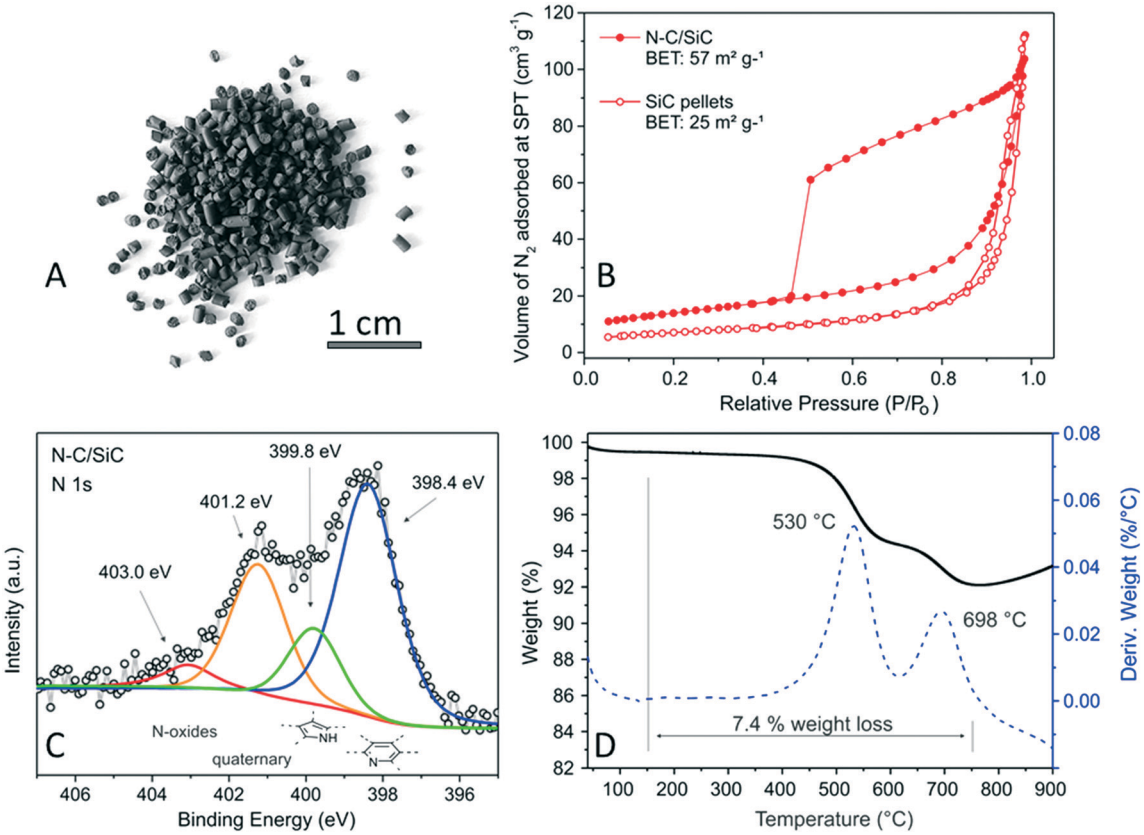

Fig. 1 (A) Digital photo of the N–C/SiC catalyst. (B) N_2 adsorption–desorption isotherm linear plot (BET) of SiC (empty dots) and N–C/SiC (full dots) samples recorded at 77 K. (C) High-resolution XPS N 1s core level region of N–C/SiC along with its relative curve fitting. (D) TG/DTG profiles of the annealed N–C/SiC sample. Weight loss is measured arbitrarily in the 150–750 °C temperature range. Operating conditions: air, 50 mL min^{-1}; heating rate: from 40 to 900 °C at 10 °C min^{-1}.

condensation in a trap (Fig. S3†). N–C/SiC samples analysed by SEM (see Fig. 6) were cooled after catalysis at a furnace temperature close to 120 °C before switching off the reagent stream and being collected for analyses. This treatment was necessary to maximize the formation of sulfur deposits at the catalysts' surfaces. All the connecting lines were wrapped with thermal tapes maintained at 140 °C in order to prevent any condensation phenomena.

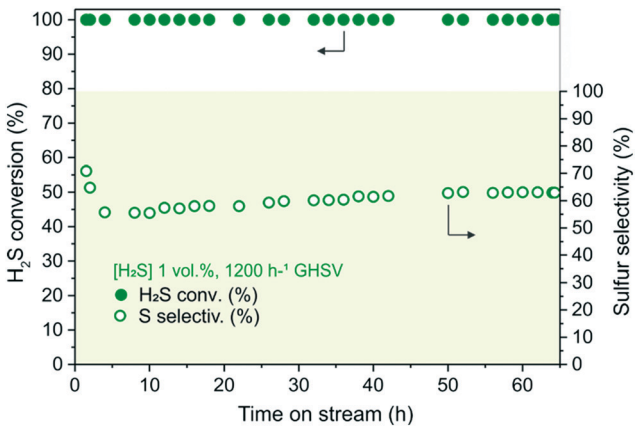

Fig. 2 Desulfurization performance on the N–C/SiC catalyst of an acid gas stream ($[H_2S]$ = 1 vol%) under toluene-free conditions. Catalysis details: N–C/SiC = 6 g (V_{cat} ~ 7.5 cm^3); O_2-to-H_2S ratio = 2.5, $[H_2O]$ = 30 vol%, He (balance); reaction temperature = 210 °C, GHSV (STP) = 1200 h^{-1}.

Results and discussion

Catalyst characterization and properties

SiC dressing with a highly N-doped mesoporous carbon phase was straightforwardly performed through two successive cycles of soaking/impregnation of SiC (10 g) in an aqueous solution of D-glucose/citric acid/ammonium carbonate (see Materials and methods for details). The wet solid underwent successive calcination steps before being annealed at 900 °C for 2 h under inert atmosphere. The as-obtained N–C/SiC composite (Fig. 1A) was first analyzed in terms of specific surface area (SSA) and pore-size distribution by N_2 physisorption analysis at the liquid N_2 temperature (77 K). As Table S1† shows, the SSA of the N–C/SiC composite is more than doubled compared to that measured on the pristine SiC support. Both materials present classical type II isothermal profiles with N–C/SiC showing a distinctive H2 hysteresis loop in the 0.4–1.0 P/P_0 range (almost absent on bare SiC – Fig. 1B and S3A†), typical of mesoporous

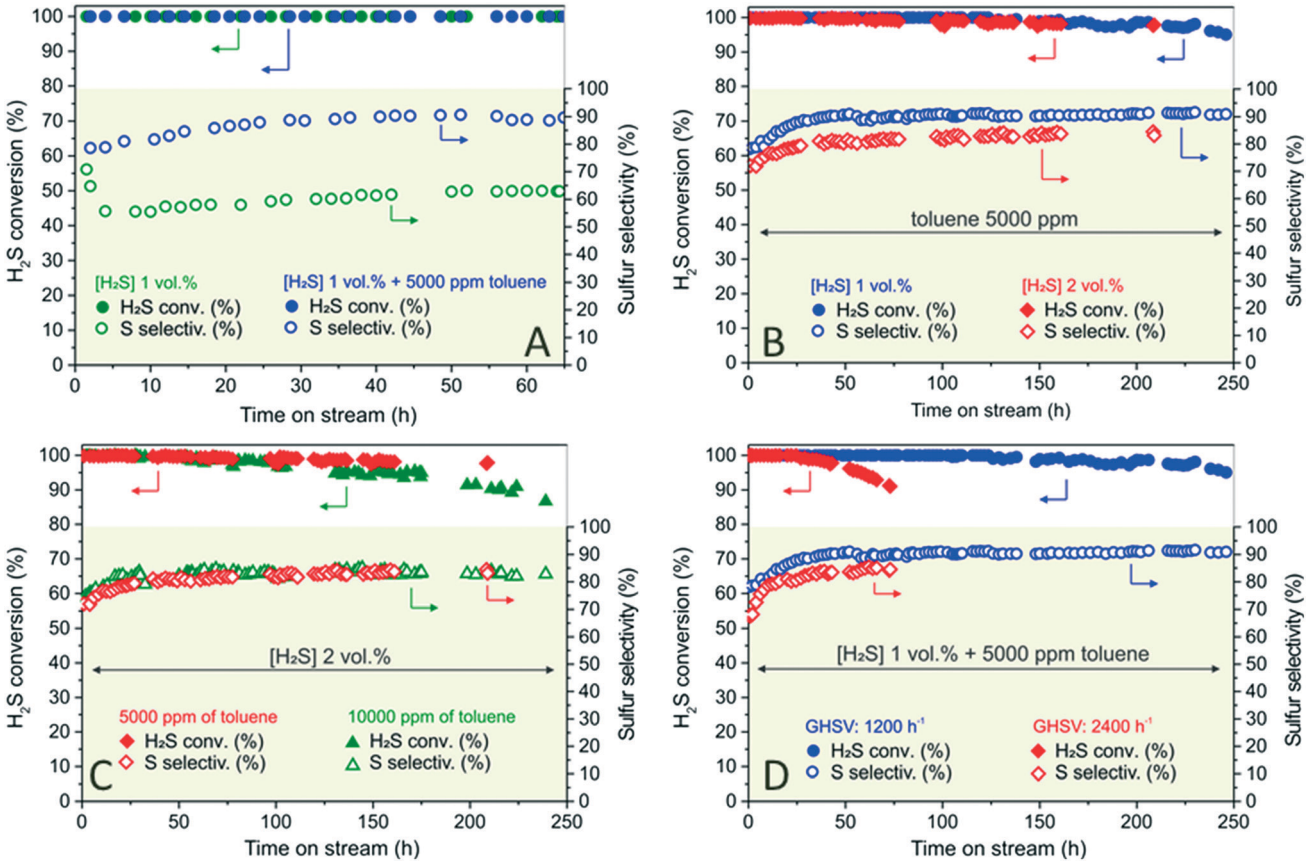

Fig. 3 (A) Comparative H_2S desulfurization runs on N–C/SiC using a sour gas ([H_2S] = 1 vol%) in the presence of toluene (5000 ppm, 0.5 vol% – blue symbols) or under toluene-free conditions (green symbols). Catalysis details: N–C/SiC = 6 g (V_{cat} ~ 7.5 cm^3); O_2-to-H_2S ratio = 2.5, [H_2O] = 30 vol%, He (balance); reaction temperature = 210 °C, GHSV (STP) = 1200 h^{-1}. (B) Long-term desulfurization tests on N–C/SiC at variable H_2S concentrations ([H_2S] = 1 vol%, blue symbols; [H_2S] = 2 vol%, red symbols) in the presence of 5000 ppm (0.5 vol%) of toluene. (C) Long-term desulfurization test on N–C/SiC in the presence of 2 vol% of H_2S under variable toluene concentrations (5000 ppm, 0.5 vol% – red symbols; 10 000 ppm, 1 vol% green symbols). Unless otherwise stated the following reaction details are common to all experiments outlined in (B) and (C): N–C/SiC = 6 g; O_2-to-H_2S ratio = 2.5, [H_2O] = 30 vol%, He (balance); reaction temperature = 210 °C, GHSV (STP) = 1200 h^{-1}. (D) Influence of GHSV (1200 h^{-1}, blue symbols; 2400 h^{-1}, red symbols) on the desulfurization of a sour gas ([H_2S] = 1 vol% + 5000 ppm, 0.5 vol% of toluene). Other catalysis details: N–C/SiC = 6 g (V_{cat} ~ 7.5 cm^3); O_2-to-H_2S ratio = 2.5, [H_2O] = 30 vol%, He (balance); reaction temperature = 210 °C.

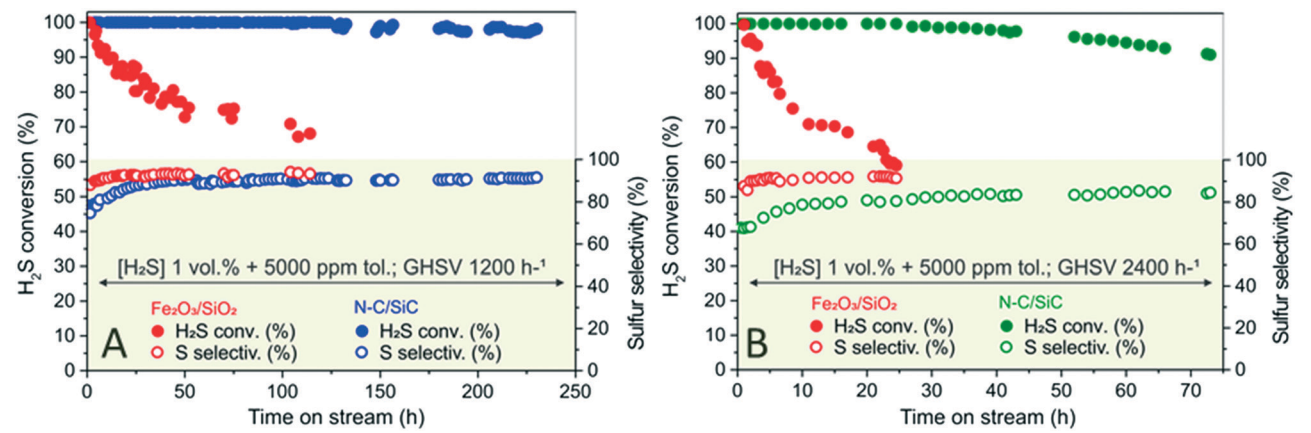

Fig. 4 Desulfurization tests on N–C/SiC and Fe_2O_3/SiO_2 catalysts at comparison with H_2S mixtures (1 vol%) containing 5000 ppm (0.5 vol%) of toluene as aromatic contaminant. (A) and (B) refer to the same desulfurization experiments conducted at variable GHSVs (A: 1200 h^{-1}; B: 2400 h^{-1}). Unless otherwise stated the following reaction details are common to all experiments outlined in (A) and (B): N–C/SiC = 6 g, $V_{cat.}$ ~ 7.5 cm^3; O_2-to-H_2S ratio = 2.5, [H_2O] = 30 vol%, He (balance); reaction temperature = 210 °C.

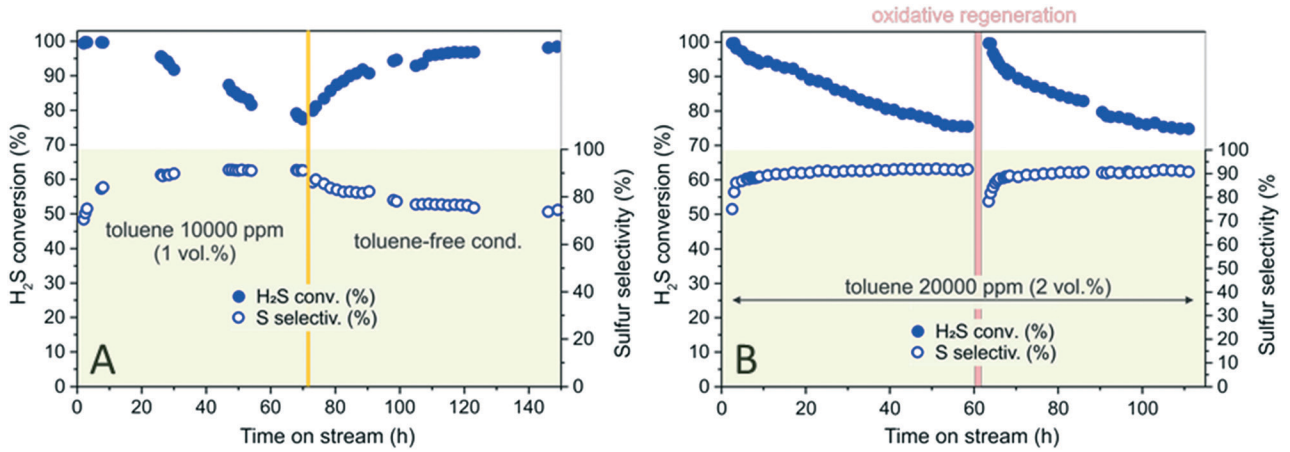

Fig. 5 (A) Desulfurization run on N–C/SiC catalyst with 1 vol% of H_2S, with and without toluene (10 000 ppm, 1 vol%). Toluene (10 000 ppm, 1 vol%) was switched off after 70 h on stream and the catalytic run is continued for a further 80 h. Other reaction details: N–C/SiC = 6 g; O_2-to-H_2S ratio = 2.5, [H_2O] = 30 vol%, He (balance); reaction temperature = 210 °C, GHSV (STP) = 1200 h^{-1}. (B) Desulfurization run on the N–C/SiC catalyst and catalyst regeneration. The desulfurization experiment was run on a mixture of H_2S (1 vol%) and toluene (20 000 ppm, 2 vol%). Catalyst regeneration after 60 h was performed at 320 °C for 2 h in a He/O_2 mixture (O_2 = 5 vol%). Other reaction details: N–C/SiC = 6 g; O_2-to-H_2S ratio = 2.5, [H_2O] = 30 vol%, He (balance); reaction temperature = 230 °C, GHSV (STP) = 1200 h^{-1}.

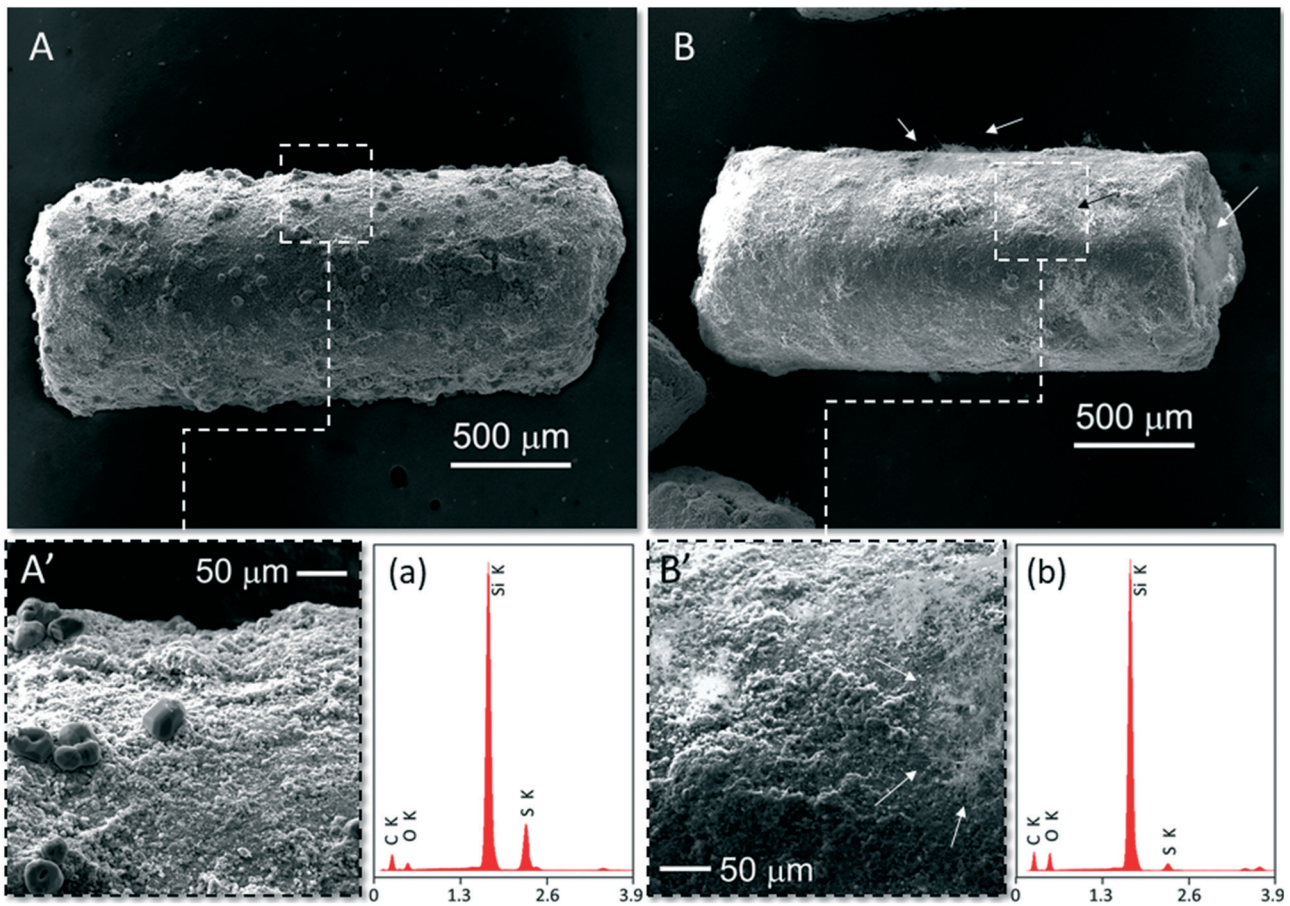

Fig. 6 SEM images at different magnifications of spent N–C/SiC catalysts (A and B) along with the respective EDS X-ray microanalyses (a and b). Spent N–C/SiC in (A) and (A′) comes from a toluene-free desulfurization run while the sample in (B) and (B′) belongs to catalysis in the presence of toluene (5000 ppm, 0.5 vol%). The SEM image of fresh N–C/SiC and its microanalysis is given in Fig. S8† for the sake of completeness.

structures featuring complex pore networks of ill-defined shape.[57] The pore-volume distribution curve recorded on N–C/SiC shows the presence of a prevalent component made up of small mesopores with a maximum pore diameter centered

around 3 nm (Fig. S4A′†). On the other hand, only larger mesopores (prevalently in the 20–40 nm range) are available on the pristine SiC support (Fig. S4A′†). SSA and pore-size distribution measured on the benchmark Fe_2O_3/SiO_2 (3 wt% Fe) did not show any major change with respect to the pristine SiO_2 support (Fig. S4B and S3B′†) except for a slight decrease of SSA likely due to a partial clogging of small micropores caused by iron nanoparticles.

As far as the basic properties of the N–C phase are concerned, the pH value of an aqueous N–C/SiC dispersion has revealed the higher basic surface character of the composite compared to that of bare SiC. Indeed, the pH of N–C/SiC lies close to pH 9.5 compared to pH 6.6 of a pristine SiC dispersion in water. To get additional insights on catalyst basic properties, a quantitative estimation of basic sites available at the catalyst surface was achieved by acid–base titration (see Materials and methods) and fixed in 0.7 mmol per g of N–C/SiC. Such a basic character of N–C/SiC was attributed to the presence of a relatively high density of surface-exposed N-sites[32,58] whose nature was carefully assessed through a high-resolution XPS N1s analysis on the composite (Fig. 1C; see also Fig. S5† for the high-resolution XPS C 1s core region and survey spectrum of the composite).

As shown in Fig. 1C, N1s peak deconvolution consists in three main components at 398.4 eV (N-pyridinic – blue line, 53.1%), 399.8 eV (N-pyrrolic – green line, 13.1%) and 401.2 eV (N-quaternary – orange line, 26.8%) together with a minor shoulder at higher binding energies (403.0 eV – red line, 7.0%) ascribed to the presence of N-oxidized species.

The N wt% loading was determined by elemental analysis as the mean value obtained over three independent runs (Table S1†) and it was fixed at 1.7%. Thermogravimetric analysis (TGA) was run in air (50 mL min^{-1}) and recorded TG/DTG profiles for N–C/SiC are outlined in Fig. 1D. The N–C/SiC annealed catalyst presents an overall weight loss (in the 150–750 °C temperature range) of 7.4%. Its TG profile shows two distinct weight losses with a maximum value at 530 and 698 °C, attributed to the stepwise combustion of "onion-veil-like" N–C phase coatings on the SiC surface. The presence of these two distinct decomposition phases is likely ascribed to a more intimate connection of the N–C phase (first coating layers) in close contact with the SiC matrix. According to the measured total weight loss in N–C/SiC (Fig. 1D) and the N wt% measured by EA (Table S1,† entry 2), the N wt% content normalized to the weight of N–C coating was calculated as 23 N wt%.

The remarkably high N-content of the N–C phase follows its high basic surface character. Finally, high-resolution STEM-EELS analyses conducted on N–C/SiC (Fig. S5A–C†) account for the high N-content in the sample along with the fairly good homogeneous N-distribution all over the scanned area.

Desulfurization runs using N–C/SiC under toluene-free conditions

N–C/SiC (6 g, $V_{cat} \sim 7.5$ cm^3) was first scrutinized as a catalyst for oxidative H_2S desulfurization under toluene-free conditions. For the sake of completeness, plain SiC was also employed as a "blank catalyst" for the process without showing any appreciable activity throughout 5 hours on stream. In a first trial, 1 vol% H_2S was flowed downward through the catalyst bed at the temperature of 210 °C under an O_2-to-H_2S ratio of 2.5 and a gas-hourly-space-velocity (GHSV) of 1200 h^{-1} (STP). As Fig. 2 shows, N–C/SiC exhibited complete desulfurization performance (>99.5% of H_2S conversion, λ = 0.67 mmol H_2S_{conv} g_{cat}^{-1} h^{-1}) with no appreciable catalyst deactivation after 60 h on stream and a sulfur selectivity lying slightly over 60%. No sulfur by-products were detected (GC analysis) at the reactor outlet except for SO_2. H_2S conversion and sulfur selectivity have been calculated according to the following equations:[59]

$$H_2S_{conv}(\%) = \frac{[H_2S]_{inlet} - [H_2S]_{outlet}}{[H_2S]_{inlet}} \times 100 \quad (4)$$

$$S_{select}(\%) = \frac{[H_2S]_{inlet} - [H_2S]_{outlet} - [SO_2]_{outlet}}{[H_2S]_{inlet} - [H_2S]_{outlet}} \times 100 \quad (5)$$

It should be noted that the sulfur selectivity decreases appreciably during the first hours on stream before approaching steady-state conditions. Such a trend is essentially ascribed to the mesoporous nature of the N–C phase (featuring relatively small mesopores – Fig. 1B and S4A′†) that hinders rapid sulfur desorption from the complex material pore network, hence fostering its undesired over-oxidation. After *ca.* 5 h on stream, the sulfur selectivity slightly increases and gradually reaches steady-state conditions after about 50 h. This period can be considered as the activation time for the catalyst stabilization.

It can be inferred that the basic surface character of the N–C phase in the composite largely contributes to the catalyst desulfurization performance. Chemically accessible basic surface sites are responsible for promoting a number of industrially relevant transformations in heterogeneous catalysis[28,52,60–62] as well as fostering a specific adsorption of Lewis/Brønsted acid molecules (*i.e.* CO_2, H_2S) for their activation/conversion. As for H_2S desulfurization, the catalyst basic surface properties are thought to create an ideal microenvironment for the generation of local H_2S gradients, determining the concentration of HS^- ions[34] and hence fostering the acid gas oxidation process.[63,64]

Steam largely contributes to the success of the process by creating a thin water film on the N–C surface, hence facilitating the dissolution of H_2S molecules and their ultimate diffusion into the material pores.[34] In addition, defect-engineered carbons, featuring "activated" C sites neighboring nitrogen dopants, are known to facilitate O_2 activation/dissociation paths.[53,65–67] The combination of these processes within the N–C phase is thought to foster the reaction between HS^- ions and adsorbed oxygen radicals, thus leading to the formation of elemental sulfur.[34] Finally, the use of SiC as N–C support ensures an ideal heat management at the catalytic sites, particularly relevant when

desulfurization is operated under harsh conditions and temperature gradients can be locally formed. The generation of local "hot spots" is generally claimed to detrimentally affect the catalyst performance (especially in terms of sulfur selectivity) as well as its lifetime on stream. In addition, iron-based desulfurization catalysts can also suffer from the excessive formation of iron sulfides that deeply affect their ultimate performance in the process. In this regard, SiC is known to mitigate or even prevent local temperature gradient formation due to its inherent thermal conductivity that makes it an ideal choice as a catalyst support within a number of highly exothermic transformations.[45,49,68–71]

Effect of toluene as acid gas contaminant on N–C/SiC desulfurization performance

Toluene was selected as a model aromatic contaminant in sour gases[72] and its effect on the N–C/SiC catalyst and its performance was thoroughly investigated under variable conditions. Fig. 3A–D outline the excellent performance of N–C/SiC under severe desulfurization conditions. They also account for the effects of the aromatic contaminant on the process activity and selectivity as well as on the catalyst stability on stream. In a first trial, a mixture of H_2S (1 vol%, O_2-to-H_2S ratio = 2.5) and toluene (5000 ppm; 0.5 vol%) was passed downward through the catalyst bed (6 g, V_{cat} = 7.5 cm^3) at 210 °C with a GHSV of 1200 h^{-1} (STP). Fig. 3A compares the N–C/SiC desulfurization performance for an acid gas stream in the presence (blue symbols) and in the absence (green symbols) of toluene as contaminant. Under these conditions, toluene gives rise only to negligible effects on H_2S conversion (at least up to 65 h on stream) as shown by the superimposable conversion profiles of the two catalytic runs (green and blue solid symbols).

On the other hand, the addition of 0.5 vol% (5000 ppm) toluene to the acid stream holds largely beneficial effects on the process selectivity. Besides preventing any initial catalyst selectivity loss, at the steady-state conditions toluene ensures a selectivity degree towards elemental sulfur up to 28% higher than that recorded for the same catalyst operated under toluene-free conditions. This highly positive feature can be rationalized on the basis of the higher solubility of formed elemental sulfur in a reagent stream containing toluene.[73] Indeed, the latter is thought to facilitate a faster sulfur removal from the material mesopores, hence preventing the occurrence of undesired over-oxidation paths (*vide infra* – characterization of spent catalysts).

It is noteworthy that a long-term catalytic desulfurization run (up to 250 h on stream – Fig. 3B, blue symbols) in the presence of 5000 ppm of toluene has shown a constantly high process selectivity (close to 90% over the entire process) and has unveiled the excellent coke resistance of N–C/SiC under severe and prolonged operating conditions. As Fig. 3B shows, catalyst deactivation starts at around 150 h with a H_2S conversion decrease of nearly 1.5% (from >99.5% to 98%) that gradually drops down to 95% (λ = 0.64 mmol H_2S_{conv} g_{cat}^{-1} h^{-1}) close to 250 h. As reported elsewhere for other processes where "catalyst coking" can deeply compromise its pristine performance,[21,62] the high resistance of N–C/SiC to coke deposits is ascribed to the metal-free nature of the oxidation catalyst along with its basic surface character that largely prevent, if not inhibit, the occurrence of undesired BTX coking phenomena.

When the process is operated at higher H_2S concentration [2 vol% H_2S, 5000 ppm (0.5 vol%) of toluene; Fig. 3B – red symbols *vs.* blue ones], H_2S conversion still maintains markedly high values, showing a moderate even though gradual catalyst deactivation (97% after 210 h, λ = 1.30 mmol H_2S_{conv} g_{cat}^{-1} h^{-1}) and a sulfur selectivity constantly close to 84% (at the steady-state conditions). The moderate loss of sulfur selectivity (<2%) is likely ascribed to the catalyst surface temperature increase when the system operates at high H_2S concentration.

When toluene concentration in the acid stream (H_2S, 2 vol%) is doubled (from 5000 ppm to 10 000 ppm), catalyst deactivation starts faster and H_2S conversion gradually decreases from 99% after 75 h (λ = 1.33 mmol H_2S_{conv} g_{cat}^{-1} h^{-1}) to 86% (λ = 1.15 mmol H_2S_{conv} g_{cat}^{-1} h^{-1}) at 240 h (Fig. 3C). It is noteworthy that sulfur selectivity is around 84% irrespective of the toluene concentration in the reagent stream (Fig. 3C – red empty symbols, 5000 ppm of toluene *vs.* green empty ones, 10 000 ppm of toluene). Such a result strengthens the high resistance of N–C/SiC towards deactivation under the adopted operating conditions (*i.e.* with higher toluene concentrations than those generally encountered in natural sour gases).[74]

The increase of GHSV (from 1200 to 2400 h^{-1} STP) on the N–C/SiC desulfurization performance for a mixture of H_2S (1 vol%, O_2-to-H_2S ratio = 2.5) containing 0.5 vol% (5000 ppm) toluene is finally illustrated in Fig. 3D. The study highlights how the higher the GHSV, the faster is the catalyst deactivation rate. Such a trend matches with a non-specific site interaction of toluene molecules on the N–C phase so that increased toluene concentrations that reach the catalyst surface (for a unit of catalyst mass per h) remain adsorbed and progressively foul the catalyst active sites, hampering the regular (and specific) H_2S and O_2 uptake. As a matter of fact, the higher the toluene concentration in the stream [from 1000 ppm (0.1 vol%) to 5000 ppm (0.5 vol%) up to 10 000 ppm (1 vol%)], the greater its effect on the catalyst deactivation rate (Fig. S7†). At the same time, higher toluene concentrations confirm a process selectivity increase.

To better appreciate the N–C/SiC performance compared to classical desulfurization systems of the state of the art, the former and the benchmark Fe_2O_3/SiO_2 catalyst were evaluated under identical conditions: H_2S mixtures (1 vol%) containing 5000 ppm (0.5 vol%) of toluene; O_2-to-H_2S ratio = 2.5, H_2O = 30 vol%, He (balance); 210 °C; GHSV 1200 h^{-1} (STP). For the sake of comparison, Fig. 4A illustrates the catalyst performance of both systems as a function of time on stream.

Despite the superimposable selectivity profiles (at the steady-state conditions) for the two catalytic systems, N–C/SiC shows its outperforming stability in run with a reduction of H_2S conversion (from >99.5% to 98%) that starts appreciably only after 125 h on stream and slightly approaches 97% at 225 h. On the other hand, Fe_2O_3/SiO_2 undergoes faster fouling of its active sites, so H_2S conversion is already reduced by 30% after 100 h on stream.

Higher GHSVs (Fig. 4B) translate into an overall reduction of the process selectivity (see also Fig. 3D) together with a faster catalyst deactivation. Nevertheless, the deactivation takes place much faster on Fe_2O_3/SiO_2 than on N–C/SiC. While H_2S conversion on Fe_2O_3/SiO_2 reduces by 40% in 25 h, it decreases by less than 10% after 75 h when the process is operated with N–C/SiC as catalyst. These outcomes highlight once again the high deactivation resistance of the N–C phase towards fouling phenomena that affect the catalyst performance in processes where formation of coke or sulfur deposits are likely to occur.

Toluene effects on N–C/SiC deactivation rate and catalyst regeneration

As discussed earlier, high GHSVs (Fig. 4B) and/or high toluene concentrations (Fig. S7†) in sour gases cause the rapid decrease of H_2S conversion over time. On the other hand, when desulfurization is operated with N–C/SiC as catalyst, the addition of toluene to the stream partially prevents the occurrence of undesired over-oxidation paths, thus ensuring higher selectivity to the process. In a model experiment operated under severe reaction conditions, sour gas desulfurization was performed over 70 h with N–C/SiC as catalyst at 210 °C, using a mixture of H_2S (1 vol%) and toluene (10 000 ppm, 1 vol%) at a GHSV of 2400 h^{-1}. As Fig. 5A shows, H_2S conversion reduces by 23% (λ = 0.52 mmol H_2S_{conv} g_{cat}^{-1} h^{-1}) within 70 h while the process selectivity constantly maintains high values (nearly 90%) over the entire process. When toluene is switched off from the stream, selectivity decreases and gradually stabilizes close to 74%. In contrast, H_2S conversion steadily increases and pristine catalyst performance is almost entirely restored (H_2S conversion = 98.5%; S selectivity = 74.4%; λ = 0.66 mmol H_2S_{conv} g_{cat}^{-1} h^{-1}) within 80 h.

In terms of process selectivity, it can be inferred that switching off toluene from the sour gas stream reduces the "solvent effect" responsible for the faster removal of elemental sulfur from the mesoporous catalyst surface. Accordingly, increased contact times between sulfur and the N–C network unavoidably foster the generation of over-oxidation by-products. As far as H_2S conversion is concerned, the gradual catalyst reactivation under toluene-free conditions accounts for the spontaneous removal of carbon–sulfur deposits (mainly formed in the presence of toluene as contaminant) already under (oxidant) desulfurization conditions. The results highlight the reversible nature of N–C/SiC deactivation caused by the presence of aromatics in the stream.

When oxidative conditions are forced into the system [oxidative regeneration, 2 h at 320 °C, He/O_2 mixture (O_2 = 5 vol%)], the catalyst performance is entirely recovered with H_2S conversion and sulfur selectivity trends that largely overlap those recorded for the pristine catalyst (Fig. 5B).

As a proof of the beneficial "solvent effect" played by toluene on the desulfurization selectivity of N–C/SiC, two catalysts recovered from distinct desulfurization cycles (40 h on stream each) carried out in the presence or in the absence of toluene (5000 ppm, 0.5 vol%) were analysed in terms of content of sulfur residues and their morphology.[75] Except for the presence of the aromatic in one of the two catalytic runs only, all other experimental conditions were kept identical [N–C/SiC = 6 g (V_{cat} 7.5 cm^3); O_2-to-H_2S ratio = 2.5, [H_2O] = 30 vol%, He (balance); reaction temperature = 190 °C, GHSV (STP) = 2400 h^{-1}].

Fig. 6 shows scanning electron microscopy (SEM) images acquired on both recovered spent catalysts (A, A′; B, B′) along with the relative energy dispersive X-ray spectroscopy (EDS) microanalyses (a and b). At first glance, the two samples show markedly high differences in terms of relative amount of sulfur deposits and their ultimate morphology.

While spent N–C/SiC obtained from desulfurization under toluene-free conditions (Fig. 6A and A′) shows the generation of large prismatic sulfur deposits, thin needles of elemental sulfur lie on the catalyst surface of the N–C/SiC sample recovered from catalysis carried out with 5000 ppm of the aromatic in the stream (Fig. 6B and B′). EDS microanalyses qualitatively show the high difference in terms of sulfur content between the two samples (Fig. 6a *vs.* b) whose quantitative estimation was given by elemental analyses (mean value calculated over three independent runs) and fixed at 5.83% and 0.37% for samples A and B, respectively.

Overall, it can be concluded that the addition of toluene to the reagents stream affects the generation of sulfur deposits and deeply modifies their morphology. Toluene promotes the rapid sulfur desorption from the catalyst surface, hence reducing its undesired accumulation at the outlet of the N–C mesoporous phase and limiting the occurrence of over-oxidation paths. Sample microanalyses and elemental analyses on the two spent catalysts are a clear proof of evidence for the above-mentioned "solvent effect" played by the aromatic in the process.

All data taken together prompted us to evaluate the beneficial effect of toluene on the process selectivity along with the high N–C/SiC deactivation resistance for low concentrations of the aromatic in the gas stream. To this purpose, 1 vol% H_2S and 1000 ppm (0.1 vol%) of toluene were passed at 1200 h^{-1} (GHSV) downward the catalyst heated at 210 °C under an O_2-to-H_2S ratio of 2.5. As Fig. 7 shows, H_2S conversion on N–C/SiC is constantly over 99.5% (λ = 0.67 mmol H_2S_{conv} g_{cat}^{-1} h^{-1}) throughout the whole long-term catalytic test (200 h), while process selectivity, after an initial

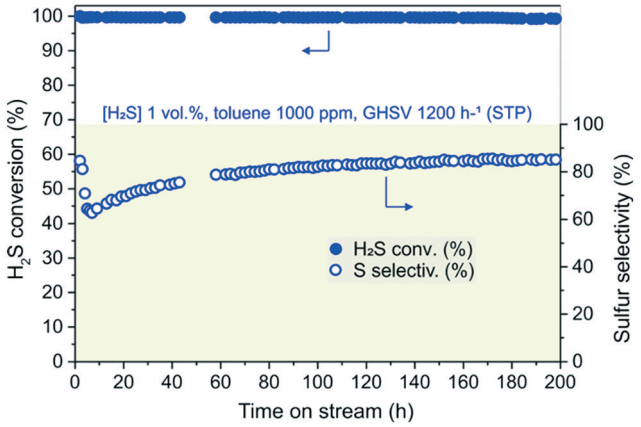

Fig. 7 Long-term desulfurization test on N–C/SiC using a sour gas ([H_2S] = 1 vol%) in the presence of toluene (1000 ppm, 0.1 vol%). Other catalysis details: N–C/SiC = 6 g (V_{cat} ~ 7.5 cm^3); O_2-to-H_2S ratio = 2.5, [H_2O] = 30 vol%, He (balance); reaction temperature = 210 °C, GHSV (STP) = 1200 h^{-1}.

fall, steadily increases and stabilizes at around 85%. As for the latter, a reduced toluene concentration (1000 ppm, 0.1 vol%) in the gas stream is not enough to balance the highly hydrophilic character of the gas stream. Thus, the latter rapidly causes pore clogging by sulfur deposits and fosters the occurrence of sulfur over-oxidation paths. Nevertheless, a prolonged catalyst exposure to the reagent stream (including toluene) restores ideal conditions for a rapid sulfur desorption from the N–C mesoporous phase and steadily increases the process selectivity.

Conclusions

The effect of variable concentrations of toluene [1000 ppm ≤ [tol] ≤ 20 000 ppm] in sour gas streams containing from 0.5 up to 2 vol% H_2S has been studied with respect to the H_2S desulfurization performance of the metal-free N–C/SiC composite. Besides its remarkable performance in the process, the study has also unveiled the higher deactivation resistance of N–C/SiC compared to classical metal-based catalysts of the state of the art. Indeed, the basic surface character of the composite together with the absence of metal active sites deeply inhibit the occurrence of undesired cracking side processes, particularly when desulfurization is operated in the presence of aromatic contaminants. It is worth noting that the combination of the mesoporous N–C active phase for the process with toluene in the gas stream has disclosed the existence of a beneficial "solvent effect" played by the aromatic on the catalyst selectivity. Indeed, toluene in the gas stream facilitates a faster removal/desorption of elemental sulfur from the mesoporous catalyst surface, hence reducing sulfur resident time in contact with the N–C network and preventing (or reducing to a large extent) the occurrence of its undesired over-oxidation paths. Evidence for the above-mentioned "solvent effect" is given by the nature of the sulfur residues (contents and morphologies) in spent catalysts recovered from desulfurization runs conducted in the presence or in the absence of toluene as contaminant. The presence of toluene in the gas stream fosters the removal of most of the sulfur residues, whose final morphology appears deeply modified: from large prismatic deposits (in the absence of toluene) to fluffy aggregates made of thin needles at the catalyst surface. As a result, the presence of low toluene concentrations (1000 ppm, 0.1 vol%) in a sour gas stream ([H_2S] = 1 vol%) can ensure high sulfur selectivity to the process (~85% at the steady-state conditions) without affecting the catalyst conversion rate *vs.* time that lies constantly over 99% for long-term runs (up to 200 h). The clear-cut step forward in using a N-rich mesoporous and metal-free active phase for the efficient and selective H_2S desulfurization reaction is proved by the comparison of N–C/SiC with a benchmark (and metal-based) system of the state of the art (Fe_2O_3/SiO_2). Overall, the developed technology offers more durable, greener and coke-resistant desulfurization catalysts for the H_2S selective treatment in gas-tail streams containing aromatics as contaminants.

Conflicts of interest

There are no conflicts to declare.

Acknowledgements

G. G. and C. P.-H. thank the TRAINER project (Catalysts for Transition to Renewable Energy Future) of the "Make our Planet Great Again" program (Ref. ANR-17-MPGA-0017) for support. The Italian team also thank the Italian MIUR through the PRIN 2017 Project MULTI-e (20179337R7) "Multielectron transfer for the conversion of small molecules: an enabling technology for the chemical use of renewable energy" for financial support to this work. The present work is also supported by the SATT-Conectus through the DECORATE project. C D.-V. and T. T.-H. thank the Vietnam National Foundation for Science and Technology Development (NAFOSTED) under grant number 104.05-2017.336 for financial support. All authors would like to thank Drs. X. Courtial and Ch. Streicher from Axens-Prosernat for technical discussion and Dr. W. Baaziz and Prof. O. Ersen for TEM analyses at IPCMS (UMR 7504). The DICP team finally acknowledges the National Natural Science Foundation of China (21606243 and 91645117), the Liao Ning Revitalization Talents Program (XLYC1907053) and the CAS Youth Innovation Promotion Association (2018220) for financial support.

Notes and references

1 (last access 28/04/2020), https://www.ucsusa.org/resources/uses-natural-gas.
2 (last access 28/04/2020), https://www.swarthmore.edu/environmental-studies-capstone/comparison-against-other-fossil-fuels.

3 J. Wieckowska, Catalytic and adsorptive desulphurization of gases, *Catal. Today*, 1995, **24**, 405–465.
4 J. S. Eow, Recovery of Sulfur from Sour Acid Gas: A Review of the Technology, *Environ. Prog.*, 2002, **21**, 143–162.
5 A. Piéplu, O. Saur, J. C. Lavalley, O. Legendre and C. Nédez, Claus Catalysis and H_2S Selective Oxidation, *Catal. Rev.: Sci. Eng.*, 1998, **40**, 409–450.
6 X. Zhang, Y. Tang, S. Qu, J. Da and Z. Hao, H_2S-Selective Catalytic Oxidation: Catalysts and Processes, *ACS Catal.*, 2015, **5**, 1053–1067.
7 D. K. Beavon, R. H. Hass and B. Muke, High recovery, lower emissions promised for Claus-plant tail gas, *Oil Gas J.*, 1979, **77**, 76–80.
8 (last access 28/04/2020), http://www.icis.com/fertilizers/sulphur/.
9 S. Faramawy, T. Zaki and A. A.-E. Sakr, Natural gas origin, composition, and processing: A review, *J. Nat. Gas Sci. Eng.*, 2016, **34**, 34–54.
10 J.-P. R. Ballaguet, M. M. Vaidya, S. A. Duval, A. Harale, A. H. Khawajah and V. V. R. Tammana, Sulfur Recovery Process for Treating Low To Medium Mole Percent Hydrogen Sulfide Gas Feeds With BTEX in a Claus Unit, Saudi Arabian Oil Company, US9593015B2, 2017.
11 A. Bahadori, *Natural Gas Processing Technology and Engineering Design*, Gulf Professional Publishing, 1st edn, 2014.
12 S. Mokhatab and W. A. Poe, *Handbook of Natural Gas Transmission and Processing*, Gulf Professional Publishing, 2012.
13 M. Jahangiri, S. J. Shahtaheri, J. Adl, A. Rashidi, H. Kakooei, A. R. Forushani, M. R. Ganjali and A. Ghorbanali, The adsorption of benzene, toluene and xylenes (BTX) on the carbon nanostructures: The study of different parameters, *Fresenius Environ. Bull.*, 2011, **20**, 1036–1045.
14 S. Sinha and A. Raj, Destruction of H_2S Contaminants (Benzene, Toluene and Xylenes) by Sulphur Dioxide in Claus Process, *Soc. Pet. Eng. J.*, 2014, 172080-MS, DOI: 10.2118/172080-MS.
15 S. Sinha, A. Raj, A. S. Al Shoaibi and S. H. Chung, Reaction Mechanism for m-Xylene Oxidation in the Claus Process by Sulfur Dioxide, *J. Phys. Chem. A*, 2015, **119**, 9889–9900.
16 S. Sinha, A. Raj, A. S. AlShoaibi, S. M. Alhassan and S. H. Chung, Toluene Destruction in the Claus Process by Sulfur Dioxide: A Reaction Kinetics Study, *Ind. Eng. Chem. Res.*, 2014, **53**, 16293–16308.
17 P. Serp, M. Corrias and P. Kalck, Carbon nanotubes and nanofibers in catalysis, *Appl. Catal., A*, 2003, **253**, 337–358.
18 D. S. Su, S. Perathoner and G. Centi, Nanocarbons for the Development of Advanced Catalysts, *Chem. Rev.*, 2013, **113**, 5782–5816.
19 H. Ba, J. Luo, Y. Liu, C. Duong-Viet, G. Tuci, G. Giambastiani, J.-M. Nhut, L. Nguyen-Dinh, O. Ersen, D. S. Su and C. Pham-Huu, Macroscopically shaped monolith of nanodiamonds @nitrogen-enriched mesoporous carbon decorated SiC as a superiormetal-free catalyst for the styrene production, *Appl. Catal., B*, 2017, **200**, 343–350.
20 J. Diao, Z. Feng, R. Huang, H. Liu, S. B. A. Hamid and D. S. Su, Selective and Stable Ethylbenzene Dehydrogenation to Styrene over Nanodiamonds under Oxygen-lean Conditions, *ChemSusChem*, 2016, **9**, 662–669.
21 H. Ba, Y. Liu, L. Truong-Phuoc, C. Duong-Viet, J.-M. Nhut, L. Nguyen-Dinh, O. Ersen, G. Tuci, G. Giambastiani and C. Pham-Huu, N-Doped Food-Grade-Derived 3D Mesoporous Foams as Metal-Free Systems for Catalysis, *ACS Catal.*, 2016, **6**, 1408–1419.
22 K. Chizari, A. Deneuve, O. Ersen, I. Florea, Y. Liu, D. Edouard, I. Janowska, D. Begin and C. Pham-Huu, Nitrogen-Doped Carbon Nanotubes as a Highly Active Metal-Free Catalyst for Selective Oxidation, *ChemSusChem*, 2012, **5**, 102–108.
23 M. Li, F. Xu, H. Li and Y. Wang, Nitrogen-doped porous carbon materials: promising catalysts or catalyst supports for heterogeneous hydrogenation and oxidation, *Catal. Sci. Technol.*, 2016, **6**, 3670–3693.
24 J. Luo, F. Peng, H. Wang and H. Yu, Enhancing the catalytic activity of carbon nanotubes by nitrogen doping in the selective liquid phase oxidation of benzyl alcohol, *Catal. Commun.*, 2013, **39**, 44–49.
25 C. Tang and Q. Zhang, Nanocarbon for Oxygen Reduction Electrocatalysis: Dopants, Edges, and Defects, *Adv. Mater.*, 2017, 1604103.
26 L. Zhang, Y. Jia, X. Yan and X. Yao, Activity Origins in Nanocarbons for the Electrocatalytic Hydrogen Evolution Reaction, *Small*, 2018, 1800235.
27 S. Zhao, D.-W. Wang, R. Amal and L. Dai, Carbon-Based Metal-Free Catalysts for Key Reactions Involved in Energy Conversion and Storage, *Adv. Mater.*, 2018, 1801526.
28 G. Tuci, J. Filippi, H. Ba, A. Rossin, L. Luconi, C. Pham-Huu, F. Vizza and G. Giambastiani, How to Teach an Old Dog New (Electrochemical) Tricks: Aziridine-Functionalized CNTs as Efficient Electrocatalysts for the Selective CO_2 Reduction to CO, *J. Mater. Chem. A*, 2018, **6**, 16382–16389.
29 X. Duan, Z. Ao, H. Sun, S. Indrawirawan, Y. Wang, J. Kang, F. Liang, Z. H. Zhu and S. Wang, Nitrogen-Doped Graphene for Generation and Evolution of Reactive Radicals by Metal-Free Catalysis, *ACS Appl. Mater. Interfaces*, 2015, **7**, 4169–4178.
30 Y. Yang, W. Zhang, X. Ma, H. Zhao and X. Zhang, Facile Construction of Mesoporous N-Doped Carbons as Highly Efficient 4-Nitrophenol Reduction Catalysts, *ChemCatChem*, 2015, **7**, 3454–3459.
31 Y. Liu, C. Duong-Viet, J. Luo, A. Hébraud, G. Schlatter, O. Ersen, J.-N. Nhut and C. Pham-Huu, One-Pot Synthesis of a Nitrogen-Doped Carbon Composite by Electrospinning as a Metal-Free Catalyst for Oxidation of H_2S to Sulfur, *ChemCatChem*, 2015, **7**, 2957–2964.
32 H. Ba, Y. Liu, L. Truong-Phuoc, C. Duong-Viet, X. Mu, W. H. Doh, T. Tran-Thanh, W. Baaziz, L. Nguyen-Dinh, J.-M. Nhut, I. Janowska, D. Begin, S. Zafeiratos, P. Granger, G. Tuci, G. Giambastiani, F. Banhart, M. J. Ledoux and C. Pham-Huu, A highly N-doped carbon phase "dressing" of macroscopic supports for catalytic applications, *Chem. Commun.*, 2015, **51**, 14393–14396.

33 C. Duong-Viet, H. Ba, Z. El-Berrichi, J.-M. Nhut, M. J. Ledoux, Y. Liu and C. Pham-Huu, Silicon carbide foam as a porous support platform for catalytic applications, *New J. Chem.*, 2016, **40**, 4285–4299.

34 F. Sun, J. Liu, H. Chen, Z. Zhang, W. Qiao, D. Long and L. Ling, Nitrogen-Rich Mesoporous Carbons: Highly Efficient, Regenerable Metal-Free Catalysts for Low-Temperature Oxidation of H_2S, *ACS Catal.*, 2013, **3**, 862–870.

35 C. Duong-Viet, L. Truong-Phuoc, T. Tran-Thanh, J.-M. Nhut, L. Nguyen-Dinh, I. Janowska, D. Begin and C. Pham-Huu, Nitrogen-doped carbon nanotubes decorated silicon carbide as a metal-free catalyst for partial oxidation of H_2S, *Appl. Catal., A*, 2014, **482**, 397–406.

36 H. Ba, C. Duong-Viet, Y. Liu, J.-M. Nhut, P. Granger, M. J. Ledoux and C. Pham-Huu, Nitrogen-doped carbon nanotube spheres as metal-free catalysts for the partial oxidation of H_2S, *C. R. Chim.*, 2016, **19**, 1303–1309.

37 Z. Yu, X. Wang, Y.-N. Hou, X. Pan, Z. Zhao and J. Qiu, Nitrogen-doped mesoporous carbon nanosheets derived from metal-organic frameworks in a molten salt medium for efficient desulfurization, *Carbon*, 2017, **117**, 376–382.

38 L. Shen, G. Lei, Y. Fang, Y. Cao, X. Wang and L. Jiang, Polymeric carbon nitride nanomesh as an efficient and durable metal-free catalyst for oxidative desulfurization, *Chem. Commun.*, 2018, **54**, 2475–2478.

39 C. Duong-Viet, H. Ba, Y. Liu, L. Truong-Phuoc, J. M. Nhut and C. Pham-Huu, Nitrogen-doped carbon nanotubes on silicon carbide as a metal-free catalyst, *Chin. J. Catal.*, 2014, **35**, 906–913.

40 C. Pham-Huu, G. Giambastiani, Y. Liu, H. Ba, L. Nguyen-Dinh and J.-M. Nhut, Method for preparing highly nitrogen-doped mesoporous carbon composites, EP3047905A1, 2016.

41 [H_2S] and [BTX] in sour gas vary in a relatively large range depending on the gas field reserve. A typical [H_2S] is assumed to be close to 0.25 vol% with a BTX content of about 2000 ppm, the latter being tentatively composed of benzene = *ca.* 900 ppm, toluene = *ca.* 750 ppm and xylene = *ca.* 400 ppm. See also ref. 12.

42 A. S. Mukasyan, in *Concise Encyclopedia of Self-Propagating High-Temperature Synthesis*, ed. I. P. Borovinskaya, A. A. Gromov, E. A. Levashov, Y. M. Maksimov, A. S. Mukasyan and A. S. Rogachev, Elsevier Inc., 2017, pp. 336–338.

43 N. Keller, C. Pham-Huu, C. Estournès and M. J. Ledoux, Low temperature use of SiC-supported NiS_2-based catalysts for selective H_2S oxidation Role of SiC surface heterogeneity and nature of the active phase, *Appl. Catal., A*, 2002, **234**, 191–205.

44 P. Nguyen, D. Edouard, J. M. Nhut, M. J. Ledoux, C. Pham and C. Pham-Huu, High thermal conductive β-SiC for selective oxidation of H_2S: A new support for exothermal reactions, *Appl. Catal., B*, 2007, **76**, 300–310.

45 M. Lacroix, L. Dreibine, B. de Tymowski, F. Vigneron, D. Edouard, D. Bégin, P. Nguyen, C. Pham, S. Savin-Poncet, F. Luck, M. J. Ledoux and C. Pham-Huu, Silicon carbide foam composite containing cobalt as a highly selective and re-usable Fischer–Tropsch synthesis catalyst, *Appl. Catal., A*, 2011, **397**, 62–72.

46 R. J. A. M. Terörde, P. J. van den Brink, L. M. Visser, A. J. van Dillen and J. W. Geus, Selective oxidation of hydrogen sulfide to elemental sulfur using iron oxide catalysts on various supports, *Catal. Today*, 1993, **17**, 217–224.

47 O. Ersen, I. Florea, C. Hirlimann and C. Pham-Huu, Exploring nanomaterials with 3D electron microscopy, *Mater. Today*, 2015, **18**, 395–408.

48 I. Florea, O. Ersen, C. Hirlimann, L. Roiban, A. Deneuve, M. Houll, I. Janowska, P. Nguyen, C. Pham and C. Pham-Huu, Analytical electron tomography mapping of the SiC pore oxidation at the nanoscale, *Nanoscale*, 2010, **2**, 2668–2678.

49 P. Nguyen and C. Pham, Innovative porous SiC-based materials: From nanoscopic understandings to tunable carriers serving catalytic needs, *Appl. Catal., A*, 2011, **391**, 443–454.

50 B. Ballesteros, G. de la Torre, C. Ehli, G. M. Aminur Rahman, F. Agulló-Rueda, D. M. Guldi and T. Torres, Single-Wall Carbon Nanotubes Bearing Covalently Linked Phthalocyanines – Photoinduced Electron Transfer, *J. Am. Chem. Soc.*, 2007, **129**, 5061–5068.

51 E. Moaseri, M. Baniadam, M. Maghrebi and M. Karimi, A simple recoverable titration method for quantitative characterization of amine-functionalized carbon nanotubes, *Chem. Phys. Lett.*, 2013, **555**, 164–167.

52 G. Tuci, L. Luconi, A. Rossin, E. Berretti, H. Ba, M. Innocenti, D. Yakhvarov, S. Caporali, C. Pham-Huu and G. Giambastiani, Aziridine-Functionalized Multiwalled Carbon Nanotubes: Robust and Versatile Catalysts for the Oxygen Reduction Reaction and Knoevenagel Condensation, *ACS Appl. Mater. Interfaces*, 2016, **8**, 30099–30106.

53 G. Tuci, C. Zafferoni, P. D'Ambrosio, S. Caporali, M. Ceppatelli, A. Rossin, T. Tsoufis, M. Innocenti and G. Giambastiani, Tailoring Carbon Nanotube N-Dopants while Designing Metal-Free Electrocatalysts for the Oxygen Reduction Reaction in Alkaline Medium, *ACS Catal.*, 2013, **3**, 2108–2111.

54 The benchmark desulfurization catalyst Fe_2O_3/SiO_2 was properly compared with our N–C/SiC system, assuming that SiC is naturally coated by a thin layer of SiO_xC_y/SiO_2 once simply exposed to air at room temperature. For literature references on SiO_xC_y/SiO_2-coated SiC see:C. Duong-Viet, H. Ba, Z. El-Berrichi, J.-M. Nhut, M. J. Ledoux, Y. Liu and C. Pham-Huu, Silicon carbide foam as a porous support platform for catalytic applications, *New J. Chem.*, 2016, **40**, 4285–4299, and refs cited therein.

55 M. A. Fahim, T. A. Alsahhaf and A. Elkilani, in *Fundamentals of Petroleum Refining*, Elsevier B.V., 2010, pp. 377–402.

56 D. D. Ebbing and S. D. Gammon, in *General Chemistry*, Houghton Mifflin Company, Boston, USA, 9th edn, 2009, ch. 223–262.

57 K. S. W. Sing, D. H. Everett, R. A. W. Haul, L. Moscou, R. A. Pierotti and J. Rouquérol, Reporting Physisorption Data For Gas/Solid Systems with Special Reference to the

Determination of Surface Area and Porosity, *Pure Appl. Chem.*, 1985, **57**, 603–619.

58 R. Arrigo, M. Hävecker, S. Wrabetz, R. Blume, M. Lerch, J. McGregor, E. P. J. Parrott, J. A. Zeitler, L. F. Gladden, A. Knop-Gericke, R. Schlögl and D.-S. Su, Tuning the Acid/Base Properties of Nanocarbons by Functionalization via Amination, *J. Am. Chem. Soc.*, 2010, **132**, 9616–9630.

59 S. W. Chun, J. Y. Jang, D. W. Park, H. C. Woo and J. S. Chung, Selective oxidation of H_2S to elemental sulfur over TiO_2/SiO_2 catalysts, *Appl. Catal., B*, 1998, **16**, 235–243.

60 X. Jin, V. V. Balasubramanian, S. T. Selvan, D. P. Sawant, M. A. Chari, G. Q. Lu and A. Vinu, Highly Ordered Mesoporous Carbon Nitride Nanoparticles with High Nitrogen Content: A Metal-Free Basic Catalyst, *Angew. Chem.*, 2009, **121**, 8024–8027.

61 S. N. Talapaneni, G. P. Mane, A. Mano, C. Anand, D. S. Dhawale, T. Mori and A. Vinu, Synthesis of Nitrogen-Rich Mesoporous Carbon Nitride with Tunable Pores, Band Gaps and Nitrogen Content from a Single Aminoguanidine Precursor, *ChemSusChem*, 2012, **5**, 700–708.

62 G. Tuci, M. Pilaski, H. Ba, A. Rossin, L. Luconi, S. Caporali, C. Pham-Huu, R. Palkovits and G. Giambastiani, Unraveling Surface Basicity and Bulk Morphology Relationship on Covalent Triazine Frameworks with Unique Catalytic and Gas Adsorption Properties, *Adv. Funct. Mater.*, 2017, **27**, 1605672.

63 Q. Chen, J. Wang, X. Liu, X. Zhao, W. Qiao, D. Long and L. Ling, Alkaline carbon nanotubes as effective catalysts for H_2S oxidation, *Carbon*, 2011, **49**, 3773–3780.

64 F. Kamali, M. M. Eskandari, A. Rashidi, M. Baghalha, M. Hassanisadi and T. Hamzehlouyan, Nanorod carbon nitride as a carbo catalyst for selective oxidation of hydrogen sulfide to sulfur, *J. Hazard. Mater.*, 2019, **364**, 218–226.

65 B. Shan and K. Cho, Oxygen dissociation on nitrogen-doped single wall nanotube: A first-principles study, *Chem. Phys. Lett.*, 2010, **492**, 131–136.

66 G. Tuci, C. Zafferoni, A. Rossin, L. Luconi, A. Milella, M. Ceppatelli, M. Innocenti, Y. Liu, C. Pham-Huu and G. Giambastiani, Chemical functionalization of N-doped carbon nanotubes: a powerful approach to cast light on the electrochemical role of specific N-functionalities in the oxygen reduction reaction, *Catal. Sci. Technol.*, 2016, **6**, 6226–6236.

67 G. Tuci, C. Zafferoni, A. Rossin, A. Milella, L. Luconi, M. Innocenti, L. Truong Phuoc, C. Duong-Viet, C. Pham-Huu and G. Giambastiani, Chemically Functionalized Carbon Nanotubes with Pyridine Groups as Easily Tunable N-Decorated Nanomaterials for the Oxygen Reduction Reaction in Alkaline Medium, *Chem. Mater.*, 2014, **26**, 3460–3470.

68 Y. Liu, I. Florea, O. Ersen, C. Pham-Huu and C. Meny, Silicon carbide coated with TiO_2 with enhanced cobalt active phase dispersion for Fischer–Tropsch synthesis, *Chem. Commun.*, 2015, **51**, 145–148.

69 Y. Liu, B. de Tymowski, F. Vigneron, I. Florea, O. Ersen, C. Meny, P. Nguyen, C. Pham, F. Luck and C. Pham-Huu, Titania-Decorated Silicon Carbide-Containing Cobalt Catalyst for Fischer–Tropsch Synthesis, *ACS Catal.*, 2013, **3**, 393–404.

70 J. Labuschagne, R. Meyer, Z. H. Chonco, J. M. Botha and D. J. Moodley, Application of water-tolerant Co/β-SiC catalysts in slurry phase Fischer–Tropsch synthesis, *Catal. Today*, 2016, **275**, 2–10.

71 X. Fan, X. Ou, F. Xing, G. A. Turlec, P. Denissenko, M. A. Williams, N. Batail, C. Pham and A. A. Lapkin, Microtomography-based numerical simulations of heat transfer and fluid flow through β-SiC open-cell foams for catalysis, *Catal. Today*, 2016, **278**, 350–360.

72 Toluene was also selected on the basis of its intermediate degree of toxicity among BTX contaminants, i.e. xylene > toluene > benzene. See: http://universulphur.com/mespon/2015_presentations/session_b/5.%20Dealing%20with%20Aromatics%20in%20the%20Sulfur%20Recovery%20Unit%20–%20Eric%20Roisin%20–%20Axens.pdf (last access 28/04/2020).

73 J. Boulegue, Solubility of Elemental Sulfur in Water at 298 K, *Phosphorus Sulfur Relat. Elem.*, 1978, **5**, 127–128.

74 C. Duncan, A. Diaz and M. Bagajewicz, *BTEX Removal from Natural Gas Streams*, Department of Chemical Engineering, University of Oklahoma, https://pdfs.semanticscholar.org/65e4/e22ad21bd7f9df086e3710d601ba101e8b3a.pdf (last access 05/02/2020), 2009.

75 Both catalytic runs were deliberately operated at a lower reaction temperature (190 °C) that is close to the sulfur dew point in order to reduce artefacts linked with the high partial pressure of sulfur in the reactor and hence maximize the generation of S deposits. This choice was taken to better benchmark the effect of sulfur dissolution caused by the presence of toluene in the reagent feed.

